Articles in PresS. Am J Physiol Lung Cell Mol Physiol (June 10, 2005). doi:10.1152/ajplung.00477.2004

FINAL ACCEPTED VERSION; LCMP-00477-2004

Sequential recruitment of neutrophils into lung and bronchoalveolar lavage fluid in LPS-induced acute lung injury

Jörg Reutershan[1) 4)], Abdul Basit [2)], Elena V. Galkina [1)3)], Klaus Ley[1) 2) 3)]

[1)] Cardiovascular Research Center, [2)] Department of Physiology and Biological Physics, and [3)] Biomedical Engineering; University of Virginia; Charlottesville, Virginia, USA, and [4)] Department of Anesthesiology and Intensive Care Medicine, University of Tübingen, Tübingen, Germany

Requests for reprints and corresponding author
Klaus Ley
University of Virginia Health System
Cardiovascular Research Center
P.O. Box 801394
Charlottesville, VA 22908-1394, USA
phone +1 (434) 243-9966
fax +1 (434) 924-2828
klausley@virginia.edu

Running head: Neutrophil migration in the lung

Abstract

Infiltration of activated neutrophils (polymorphonuclear leukocytes; PMN) into the lung is an important component of the inflammatory response in acute lung injury. The signals required to direct PMN into the different compartments of the lung have not been fully elucidated. In a murine model of LPS-induced lung injury, we investigated the sequential recruitment of PMN into the pulmonary vasculature, lung interstitium, and alveolar space. Mice were exposed to aerosolized LPS and bronchoalveolar lavage fluid (BAL) and lungs were harvested at different time points. We developed a flow cytometry-based technique to assess in-vivo trafficking of PMN in the intravascular and extravascular lung compartments. Aerosolized LPS induced consistent PMN migration into all lung compartments. We found that sequestration in the pulmonary vasculature occurred within the first hour. Transendothelial migration into the interstitial space started one hour after LPS-exposure and increased continuously until a plateau was reached between twelve and 24 hours. Transepithelial migration into the alveolar airspace was delayed, as the first PMN did not appear until two hours after LPS, reaching a peak at 24 hours. Transendothelial migration was partially and transepithelial migration was completely inhibited by pertussis toxin, indicating involvement of Gαi-coupled receptors. These findings confirm LPS-induced migration of PMN into the lung. For the first time, distinct transmigration steps into the different lung compartments are characterized in vivo.

Key words: Acute lung injury; Polymorphonuclear Leukocytes; Pulmonary circulation; Chemokines

Introduction

Acute lung injury (ALI) and acute respiratory distress syndrome (ARDS) are characterized by a disturbance of the alveolar-capillary barrier associated with several clinical disorders. There is no specific therapy, and the mortality of this disease is still high. Our current understanding of the molecular mechanisms of ALI/ARDS has recently been described as “embryonic at best” (27).

Migration of activated PMN plays a key role in development of ALI and ARDS (1). Here, we investigate the sequential migration steps from blood to air space (intravascular sequestration – transendothelial migration – transepithelial migration).

A variety of stimuli induce PMN migration into the lung. Endotoxin of Gram-negative bacteria (lipopolysaccharide; LPS) induces a range of inflammatory responses. Toll-like receptor 4 (TLR4) is the most important cellular receptor for LPS. LPS stimulates the response to chemoattractants and increases PMN migration at sites of inflammation (14). TLR4 is essential for LPS-induced PMN migration into the lung as shown by the absence of a response in TLR4-deficient mice (3). In the lung, the response to LPS is regulated by radioresistant cells, most likely endothelial cells (2) or alveolar macrophages (28).

The administration of LPS alone might not reflect the whole complexity of the human disease, because it does not consider preexisting diseases, fluid resuscitation, or mechanical ventilation (36). However, infections with gram-

negative bacteria and exposure to their predominant pathogenic component play a key role in both development and outcome of ARDS (26).

PMN trafficking into the vascular compartment of the lung, also known as “margination” (9), and into the bronchoalveolar space has been studied extensively in various models of acute lung injury. Adhesion molecules and CXC chemokines have been shown to be involved. CXC chemokines, such as CXCL8 (IL-8), promote PMN migration into the alveolar compartment (29), and pertussis toxin-dependent chemokine receptors are essential for PMN infiltration in the lung (4; 42). Selectins and integrins are thought to be required for PMN sequestration into the vascular compartment (6). However, results from studies using monoclonal antibodies and mutant mice have yielded conflicting results (10). The importance of investigating each step of PMN migration in the lung has been emphasized recently (8).

Methodological limitations complicate the assessment of PMN trafficking in the lung. Most studies employ indirect parameters to assess PMN trafficking in the lung. For instance, the drop in circulating PMN counts in response to an inflammatory stimulus was used to estimate PMN sequestration in the lung vasculature (6; 31). However, recruitment to other organs might occur at the same time. Ex-vivo labeling of murine PMN might result in neutrophil activation that makes results uninterpretable (7). Myeloperoxidase activity in the lung is often measured to estimate PMN infiltration, but this technique is not able to distinguish between intravascular and interstitial PMN. Intravital microscopy of the pulmonary microcirculation has recently become available in mice (35; 39)

and will promote insights into the interactions between leukocytes and endothelium. However, this technique is technically challenging because of the respiratory movement, requires mechanical ventilation, and allows observation of only the most superficial lung capillaries, which may not be representative of the whole lung. Morphometric analysis, such as electron microscopy (16), is useful, but remain semi-quantitative, time-consuming and expensive.

In this study, we developed a flow cytometry based approach to assess the different steps of PMN trafficking in a murine model of LPS-induced acute lung injury. PMN accumulation in the pulmonary vasculature, transendothelial migration into the interstitium, and transepithelial migration from the interstitium into the airspace occurred as a sequential process in a time dependent manner. Our findings improve the current understanding of neutrophil recruitment into the inflamed lung and airways in a model that mimics some aspects of ALI/ARDS.

Methods

Mice

Wild type male C57Bl/6 mice were obtained from Jackson Labs (Bar Harbor, ME). All animal experiments were approved by the Animal Care and Use Committee of the University of Virginia. Mice were eight to twelve weeks of age.

Antibodies for flow cytometry

Rat anti-mouse antibodies for flow cytometry were obtained from Pharmingen (anti-CD45; clone 30-F11), Caltag (anti-7/4; recognizing the 7/4 antigen on

murine neutrophils), and eBioscience (anti-TER-119; recognizing glycophorin A-associated TER-119 on cells of the erythroid lineage). Anti-mouse GR-1 antibody was purified from supernatant of the GR-1 hybridoma (ATCC) by the biomolecular facility of University of Virginia. GR-1 was labeled with a staining kit following the manufacturer's directions (Alexa Fluor 633, Molecular Probes). Appropriate rat anti-mouse IgG2a and IgG2b (Pharmingen) were used as isotype controls.

Murine model of acute lung injury

Aerosolized LPS was utilized to induce PMN-infiltration in the lung (40). Besides PMN-migration, LPS-inhalation is known to induce the expression of various inflammatory mediators such as chemokines and adhesion molecules. LPS has also been shown to increase airway resistance (24). Up to four mice were exposed simultaneously to aerosolized LPS in a custom-built cylindrical chamber (20cm in length; 9cm in diameter) connected to an air nebulizer (MicroAir, Omron Healthcare, Vernon Hills, IL). This system produced particles in the range of one to five µm. LPS from *Salmonella enteritidis* (Sigma Co., St. Louis, MO) was dissolved in 0.9% saline (500µg/ml) and mice were allowed to inhale LPS for 30 minutes. One side of the chamber was connected to a vacuum pump and a constant flow rate of 15 ml/min was ensured using a flow meter (Gilmont Instruments, Barrington, Illinois).

PMN counts in bronchoalveolar lavage fluid (BAL) and lung tissue

At different time after LPS exposure, mice were anesthetized with an intraperitoneal injection of ketamine (125 mg/kg; Sanofi Winthrop Pharmaceuticals, New York, NY), xylazine (12.5 mg/kg; Phoenix Scientific, St. Joseph, MO) and atropine sulfate (0.025 mg/kg; Fujisawa, Deerfield, IL). The pulmonary circulation was rinsed by injection of 10ml of PBS at 25 cmH_2O into the beating right ventricle after the inferior vena cava had been cut to allow exsanguination. This was done to remove non-adherent PMN from the pulmonary vessels. The trachea was cannulated (22 GA Insyte, Becton Dickinson) and 1ml of PBS was infused intratracheally and withdrawn. This procedure was repeated six times, resulting in a total volume of 7 ml. BAL fluid was centrifuged for 5 minutes at 300g. The pellet was resuspended in 1ml buffer (1% BSA and 0.1% sodium azide in PBS), and a 10µl aliquot was used for cell count with a hemocytometer (Trypan Blue exclusion).

After performing BAL, lungs were harvested en bloc. Mediastinal tissue was removed, lungs were minced and digested with 125 U/ml collagenase type XI, 60 U/ml hyaluronidase type I-s and 60 U/ml DNAse1 (all Sigma) at 37°C for 30 min. Digested lungs were passed through a 70 µm cell strainer (BD Falcon, Bedford, MA) and the resulting cell suspension was centrifuged for 10 minutes at 300g. The pellet was lyzed using 0.83% NH_4Cl to remove erythrocytes, and centrifuged again. Pellet was resuspended in buffer and cells were counted with a hemocytometer.

PMN were identified by 1) their typical appearance in the FSC/SSC, 2) by their expression of $CD45^+$, and 3) by two independent PMN-markers, 7/4 and GR-1 (19), and the absolute numbers of leukocytes ($CD45^+$) and PMN were calculated. Appropriate isotypes were used to set the gates. All studies were performed on a FACS Calibur, Becton Dickinson (San Jose, CA), and data were analyzed with FlowJo software (Tree Star, Ashland, OR). To confirm the presence of PMN within the different populations as defined by flow cytometry, we sorted both $7/4^+GR\text{-}1^+$ and $7/4^+GR\text{-}1^-$ cells (FACS Vantage, Becton Dickinson) and characterized them morphologically by cytospin (Diff Quick staining; IMEB Inc, IL).

In-vivo trafficking experiments

Dialyzed Alexa 633-labeled rat anti-mouse GR-1 (10µg) antibody was injected i.v. and allowed to circulate for five minutes to bind to intravascular PMN. After five minutes, mice were euthanized. BAL was obtained as described above, and the lungs were homogenized in the presence of excess unlabeled anti-GR-1 to prevent possible binding of excess Alexa 633-GR-1 to extravascular PMN. Cell suspensions from BAL and lung tissue were made and cells were counted in a hemocytometer.

Non-perfused or occluded vessels in the lung might result in trapped neutrophils, not accessible for the injected antibody. This would lead to an underestimation of PMN counts in the intravascular compartment. Non-perfused / occluded vessels contain white and red blood cells. To assess the significance of this phenomenon in our model, a monoclonal antibody to the TER-119 antigen on erythrocytes was

injected i.v. (TER-119; eBioscience, San Diego, CA). This 52-kDa molecule is associated with glycophorin A on cells of the erythroid lineage (22). Five minutes after injection, blood and lungs were harvested. Erythrocytes were defined by their typical appearance in the forward-sideward scatter and the amount of TER-119^+ erythrocytes in each organ was expressed as percentage of total erythrocytes by flow cytometry. To assess the effect of i.v. injection of anti-GR-1 on peripheral PMN counts, in some experiments, blood was withdrawn from the tail vein and blood counts were performed before and ten minutes after antibody injection using an automatic cell counter (Hemavet, Drew Scientific, Dallas, TX). In all experiments, animals exposed to aerosolized saline served as control.

Cytospin of BAL

In some experiments, cytospins of the BAL (without LPS-treatment and 24 hours after LPS-inhalation) were performed using a cytocentrifuge (Shandon, Southern Sewickley, PA). The cytospun cells were Giemsa stained, air-dried and coverslipped.

Lung permeability

To confirm lung injury in our LPS inhalation model, we determined microvascular permeability using the Evans blue dye extravasation technique. Evans blue (20mg/kg; Sigma-Aldrich) was injected i.v. 30 minutes prior to euthanasia. Lungs were perfused through the spontaneously beating right ventricle. Lungs were removed and Evans blue was extracted as described previously (32). The absorption of Evans blue was measured at 620 nm and corrected for the

presence of heme pigments: A_{620} (corrected) = A_{620} - (1.426 x A_{740} + 0.030) (45). Extravasated Evans blue was determined 6 hours after LPS or saline inhalation and calculated against a standard curve (micrograms Evans blue dye per gram lung).

PTx pretreatment

Chemokines have been shown to regulate PMN migration in the lung (42). To block chemokine-mediated PMN migration, some mice received tail vein injections of 4 µg of Pertussis toxin (PTx) from *Bordetella pertussis* (Lyophilized powder, Sigma) 30 minutes prior to LPS exposure. This dose completely inhibits Gα1-mediated signaling (41). PTx was dissolved in physiological saline. PMN in lung and BAL were assessed 14 hours after LPS exposure. In addition, a dose-response-curve was established for each lung compartment 12 hours after LPS exposure (0, 0.04, 0.4, or 4 µg PTx / mouse).

Statistical analysis

Data were analyzed using Excel software package (Microsoft). PMN counts were compared with the paired Student's t-Test. $P < 0.05$ was considered statistically significant. Data were expressed as the mean ± SEM.

Results

LPS-induced PMN recruitment into lung and BAL

LPS-inhalation induced a time-dependent PMN recruitment into lung and BAL (Figure 1). In the lung, significant numbers of leukocytes (CD45+ cells) were present even before LPS administration, and their numbers increased only moderately from four to a maximum of nine million cells at four hours after LPS. Neutrophils were also present in resting lungs (approximately one million per mouse), consistent with the concept of a physiologically marginated pool in the pulmonary vasculature. Lung neutrophil numbers reached more than six million cells/mouse at four hours of LPS administration, which is several-fold more than the total number of all circulating neutrophils consistent with a previously described release of PMN from the bone marrow (37; 46). At the peak of the response, neutrophils accounted for 74 ± 7% of all leukocytes in the lung.

No PMN were observed in the BAL at 0h. PMN recruitment into the airspace was delayed, and the first PMN did not appear until two hours. Between two and four hours, neutrophil recruitment was very pronounced. After 48 hours, cell counts in BAL were reduced, but did not reach baseline.

In-vivo GR-1 labeling

In the lung homogenate, GR-1 labeling was utilized to distinguish between PMN derived from the pulmonary vasculature (GR-$1^{+}7/4^{+}$) and PMN derived from interstitial space (GR-$1^{-}7/4^{+}$). We assessed the PMN labeling five minutes after injection of anti-GR-1 antibody. We found that almost all blood PMN

(99.2 ± 0.4%) had been stained with GR-1 five minutes after antibody injection (Figure 2A and B; table 1). To test whether GR-1 antibody was leaking into the BAL, GR-1 labeling of PMN in BAL ($CD45^+7/4^+$) was assessed at different time points after LPS-exposure, five minutes after antibody injection. No $GR\text{-}1^+$ cells were found in BAL. When GR-1 antibody was added after BAL harvesting, all PMN were $GR\text{-}1^+$ (positive control) (Figure 2C and D; table 1). $GR\text{-}1^+$ PMN did not appear in the BAL until 4h after antibody injection (data not shown).

Although all circulating PMN were shown to be $GR\text{-}1^+$, potential non- or poorly perfused areas of the pulmonary vasculature might be inaccessible for an intravenously injected antibody. This would result in an underestimation of the intravascular or an overestimation of the interstitial PMN concentration in the lung, respectively. This effect might occur particularly in the injured lung. We therefore labeled erythrocytes by i.v. injection of an antibody to the TER-119 antigen of red blood cells intravenously, 24 hours after LPS exposure. Red blood cells are not found in the lung interstitium or BAL (5). The amount of $TER\text{-}119^+$ cells in all erythrocytes were then determined in both blood and lung homogenate. Five minutes after injection, we found 98.8% of all blood erythrocytes to be $TER\text{-}119^+$. At the same time, 97.7% of all erythrocytes were $TER\text{-}119^+$ in the lung homogenate indicating that the injected antibody is able to bind to almost all red cells in the pulmonary vasculature.

Effect of anti-GR-1 antibody on PMN blood counts

GR-1 antibody can induce a severe neutropenia when given at high doses (33). Therefore, we performed peripheral blood counts before and ten minutes after

antibody injection. GR-1 injection did not affect blood PMN counts at the concentration used in our study (0.89 ± 0.14x10^3/µl before, 0.86 ± 0.16 x10^3/µl after injection; p = 0.90).

In-vivo trafficking experiments

We assessed the concentration of PMN in the different lung compartments at 0, 1, 2, 4, 12, and 24 hours after LPS-exposure. At each time point, anti-GR-1 antibody was injected five minutes prior to euthanasia. PMN were identified by flow cytometry (FSC/SSC-gate; $CD45^+7/4^+$) and GR-1 was utilized to distinguish between intravascular ($GR\text{-}1^+$) and interstitial ($GR\text{-}1^-$) PMN (Figure 3). Both populations predominantly consisted of PMN as confirmed morphologically by cytospins ($7/4^+$/$GR\text{-}1^+$: 99% PMN; $7/4^+GR\text{-}1^-$: 97% PMN; data not shown). At 0h, 86% of all PMN were found in the vascular compartment. LPS induced PMN accumulation in the pulmonary vasculature. Both absolute and relative PMN counts increased rapidly until a peak was reached after four hours. After four hours, PMN counts in the vasculature decreased and returned to baseline at 24 hours after LPS-exposure (Figure 3A).

PMN concentration in both interstitium and bronchoalveolar lavage was negligible at 0h. After 4h, 33% of all pulmonary PMN were found in the interstitium. At the same time, PMN represented 91% of all cells in the BAL (Figure3B). After 24h, the majority of PMN (78%) in the lung were found in the extravascular space. Note that PMN in BAL appear $GR\text{-}1^-$ as the GR-1 antibody injected five minutes before euthanasia remains confined to the vasculature. In control animals, saline inhalation induced a mild PMN accumulation in the

pulmonary vasculature. No migration into the interstitium or into the alveolar airspace was observed in these mice (data not shown).

Kinetics of transendothelial and transepithelial PMN migration

Interstitium and airspace were free of PMN at 0h. Transendothelial migration into the interstitial space started one hour after LPS-exposure and increased continuously. After twelve hours, the majority of PMN in the lung were now found extravascular (interstitium and airspace) (Figure 4). Until two hours, the intravascular accumulation outpaced the neutrophil accumulation in the extravascular space so that the proportion of extravascular PMN did not change. By contrast, at four hours the rate of accumulation of intravascular neutrophils slowed and extravascular PMN accounted for 33% of all neutrophils in the lung.

The kinetics of neutrophil recruitment into the BAL was different in that no cells were found at one hour and only a very small number (130.000 per mouse) at two hours, after which time neutrophil numbers increased rapidly and then followed the number of interstitial neutrophils with a delay of about two hours.

The appearance of PMN in the BAL was confirmed by cytospin. Cytospins of BAL were analyzed in untreated mice and in mice 24 hours after LPS-inhalation. The predominant cells in BAL of untreated mice were alveolar macrophages (Figure 4, left inset). As expected, PMN dominated the cell population 24 hours after LPS-exposure (Figure 4, right inset).

Lung permeability

Vascular leakage was determined to confirm lung injury in our LPS inhalation model. 6 hours after LPS inhalation, Evans blue extravasation was significantly higher compared to saline inhalation (66.2 ± 6.2 vs. 29.3 ± 3.7 µg per g lung; $p = 0.002$) (Figure 5).

PTx treatment

In some mice, 4µg of PTx (41) was injected i.v. 30 minutes prior to LPS challenge. Lungs and BAL were harvested 14 hours after LPS-exposure, and anti-GR-1 was injected five minutes prior to euthanasia to distinguish between intravascular and interstitial PMN. LPS induced a significant PMN migration into all three lung compartments. Mice pretreated with PTx exhibited a normal PMN sequestration into the pulmonary vasculature but showed a reduced PMN migration into the lung interstitium ($0.5 \pm 0.1 \times 10^6$ vs. $2.7 \pm 0.4 \times 10^6$; $p < 0.01$) (Figure 6A and B). Accordingly, almost no PMN were found in the alveolar airspace at 14 hours after LPS ($0.3 \pm 0.01 \times 10^6$ vs. $2.8 \pm 0.3 \times 10^6$; $p < 0.01$) (Figure 6B). The inhibitory effect of PTx was dose-dependent as shown in Figure 7. This suggests that Gαi is involved at least in transendothelial migration from blood space to interstitium and possibly also in transepithelial migration into the alveolar airspace.

Discussion

In a LPS-induced model of acute lung injury, the sequential migration of PMN into the different compartments of the lung was explored. Using a new and quantitative flow cytometry-based technique, we show that LPS-inhalation induced a rapid PMN sequestration in the pulmonary vasculature. Migration into the lung interstitium was observed within one hour after LPS-exposure while transepithelial migration was delayed. Pertussis toxin sharply reduced migration into the interstitium and into the alveolar airspace but did not affect vascular accumulation.

Methodological considerations

When using antibody injection to identify intravascular neutrophils in the lung, the antibody is required to reach all PMN in this compartment. We found a complete GR-1 labeling of all PMN in the systemic circulation. Additionally, the accessibility of the pulmonary vasculature was successfully tested using a marker for erythrocytes.

Even within five minutes, the GR-1 antibody might leak and stain extravascular PMN. In our studies, GR-1^+ PMN did not appear until four hours after antibody injection in the BAL, indicating that the antibody did not reach alveolar airspace. To test for antibody leakage into the interstitium, we injected a higher (10-fold) dose of GR-1 that should increase the amount of leaked antibody and lead to an increased fraction of labeled PMN. No such increase was observed in our experiments (data not shown). Finally, a possible endothelial leakage should

increase as the LPS-induced alveolo-capillary damage proceeds over time leading to a continuously rising overestimation of the intravascular PMN-fraction. However, intravascular PMN-concentration peaks at 4h after LPS, while PMN-concentration in the interstitium increases at this time (Figure 4). Taken together, antibody leakage into the interstitium does not appear to play a major role in our study.

Alveolar PMN are removed by bronchoalveolar lavage. Inaccessible airways might exist, particularly in the inflamed lung, leaving ($GR\text{-}1^-$) PMN in the airspace. This might result in an overestimation of the PMN counts in the interstitial compartment. However, significant contribution of alveolar PMN to the fraction of $GR\text{-}1^-$ PMN would be reflected by an either constant or increased ratio between interstitial and total extravascular (interstitial + alveolar) PMN over time. In fact, the fraction of interstitial PMN in all extravascular PMN decreases over time (Figure 4). In addition, PMN counts in the interstitium reach a plateau after twelve hours, while the PMN concentration in the airspace still arises. Therefore, this effect does not significantly contribute to the results.

Investigating PMN migration in the lung

Although the lung offers a unique system to study cell migration, molecular mechanisms are still largely unknown.

Transendothelial migration from the vasculature into the lung interstitium was not measured in earlier studies. Indirect measurements, such as a drop in PMN blood counts or lung MPO activity are not suitable to study the first important migration step. Current knowledge about the interaction between PMN and

pulmonary endothelium derives mostly from in-vitro studies using endothelial cell lines (25; 30). Attempts were recently made to mimic the alveolo-capillary barrier in an in-vitro system more realistically (20). It remains to be shown whether this method will provide insight into pulmonary PMN migration.

Our flow cytometry based approach is able to reflect many aspects of PMN trafficking in vivo, including the presence of a physiological marginated pool (9), accumulation after challenge as well as the different migration steps into the alveolar airspace and the LPS-induced release of PMN from the bone marrow (37; 46).

Kinetics of PMN trafficking

Several studies addressed the kinetics of PMN trafficking in the lung. Most of them focused on the initial retention in the pulmonary capillaries. Mathematical models (18; 21), multiple-indicator techniques (38), injection of labeled PMN (17), as well as isolated lung models have been developed to describe PMN retention in the lung. PMN sequestration in the pulmonary vasculature in response to various inflammatory stimuli, such as live bacteria (13), complement fragments (31), MIP-2 (16), or LPS (2) occurs rapidly within a few minutes. PMN migration into the lung was detected as early as one to two hours after injection of C5-fragment or *Escherichia coli* as assessed by radiolabeled PMN (11; 15). PMN infiltration into the BAL has been shown to be delayed for up to six hours (12; 13; 43; 44). We found evidence of PMN migration into the alveolar airspace starting after two hours with a peak between 12 and 24 hours. At 4h, vascular PMN accumulation reached its maximum indicating that PMN recruitment from the

peripheral circulation was balanced by migration into the interstitium and the alveolar airspace at an equal rate. The interstitial space was holding a significant number of PMN during the migration process indicating that this space functions as a discrete compartment after an inflammatory stimulus.

Leukocyte-endothelial interactions are essential for the PMN recruitment to the lung (34). The engagement of molecules required for PMN recruitment, such as adhesion molecules or chemokines, varies among different inflammation models. There is good evidence that distinct signals are required for PMN to migrate through the different barriers and even one single mediator can affect the migration steps differentially. For instance, nitric oxide induces vascular PMN sequestration in a murine model of sepsis but attenuates migration into the alveolar airspace (35). In our study, pertussis toxin was able to block both transendothelial and transepithelial migration. However, the vascular accumulation was largely unaffected, indicating that chemokine receptor signaling is not required for neutrophil arrest in the pulmonary circulation. It has been previously suggested that chemokines and adhesion molecules contribute both equally to PMN arrest in the systemic microcirculation (41). It remains to be shown whether this mechanism applies in the lung as well.

The delay of transepithelial PMN migration in PTx-treated mice supports the hypothesis that a distinct signal is required for PMN to advance from the lung interstitium into the alveolar airspace. Interestingly, PMN crossing the epithelial barrier seem to be pivotal for inducing lung damage associated with an increase in mortality (23).

Our data establish the first quantitative method to monitor neutrophil migration from blood to lung interstitium to alveolar airspace. Vascular sequestration occurred immediately after LPS challenge, while transendothelial and transepithelial migration into the airspace were delayed. In acute lung injury, the lung interstitium holds a significant amount of PMN during the migration process. Distinguishing intravascular and interstitial PMN in-vivo facilitates new opportunities to study the regulation of PMN migration in the lung.

This study was supported by fortüne grant of the Medical Faculty of the University of Tübingen (1099-1-0) to J.R. and by National Institutes of Health (NIH) grant HL73361 to K.L.

References

1. **Abraham E**. Neutrophils and acute lung injury. *Crit Care Med* 31: S195-S199, 2003.

2. **Andonegui G, Bonder CS, Green F, Mullaly SC, Zbytnuik L, Raharjo E and Kubes P**. Endothelium-derived Toll-like receptor-4 is the key molecule in LPS-induced neutrophil sequestration into lungs. *J Clin Invest* 111: 1011-1020, 2003.

3. **Andonegui G, Goyert SM and Kubes P**. Lipopolysaccharide-induced leukocyte-endothelial cell interactions: a role for CD14 versus toll-like receptor 4 within microvessels. *J Immunol* 169: 2111-2119, 2002.

4. **Belperio JA, Keane MP, Burdick MD, Londhe V, Xue YY, Li K, Phillips RJ and Strieter RM**. Critical role for CXCR2 and CXCR2 ligands during the pathogenesis of ventilator-induced lung injury. *J Clin Invest* 110: 1703-1716, 2002.

5. **Burns AR, Smith CW and Walker DC**. Unique structural features that influence neutrophil emigration into the lung. *Physiol Rev* 83: 309-336, 2003.

6. **Burns JA, Issekutz TB, Yagita H and Issekutz AC**. The beta2, alpha4, alpha5 integrins and selectins mediate chemotactic factor and endotoxin-enhanced neutrophil sequestration in the lung. *Am J Pathol* 158: 1809-1819, 2001.

7. **Cotter MJ, Norman KE, Hellewell PG and Ridger VC**. A novel method for isolation of neutrophils from murine blood using negative immunomagnetic separation. *Am J Pathol* 159: 473-481, 2001.

8. **Doerschuk CM**. NO and Neutrophils during Sepsis: NO says "Yes" to Sequestration but "No" to Migration. *Am J Respir Crit Care Med* 170: 205-206, 2004.

9. **Doerschuk CM, Allard MF, Martin BA, MacKenzie A, Autor AP and Hogg JC**. Marginated pool of neutrophils in rabbit lungs. *J Appl Physiol* 63: 1806-1815, 1987.

10. **Doerschuk CM, Quinlan WM, Doyle NA, Bullard DC, Vestweber D, Jones ML, Takei F, Ward PA and Beaudet AL**. The role of P-selectin and ICAM-1 in acute lung injury as determined using blocking antibodies and mutant mice. *J Immunol* 157: 4609-4614, 1996.

11. **Doherty DE, Downey GP, Worthen GS, Haslett C and Henson PM**. Monocyte retention and migration in pulmonary inflammation. Requirement for neutrophils. *Lab Invest* 59: 200-213, 1988.

12. **Downey GP, Worthen GS, Henson PM and Hyde DM**. Neutrophil sequestration and migration in localized pulmonary inflammation. Capillary localization and migration across the interalveolar septum. *Am Rev Respir Dis* 147: 168-176, 1993.

13. **Doyle NA, Bhagwan SD, Meek BB, Kutkoski GJ, Steeber DA, Tedder TF and Doerschuk CM**. Neutrophil margination, sequestration, and emigration in the lungs of L-selectin-deficient mice. *J Clin Invest* 99: 526-533, 1997.

14. **Fan J and Malik AB**. Toll-like receptor-4 (TLR4) signaling augments chemokine-induced neutrophil migration by modulating cell surface expression of chemokine receptors. *Nat Med* 9: 315-321, 2003.

15. **Gao X, Xu N, Sekosan M, Mehta D, Ma SY, Rahman A and Malik AB**. Differential role of CD18 integrins in mediating lung neutrophil sequestration and increased microvascular permeability induced by Escherichia coli in mice. *J Immunol* 167: 2895-2901, 2001.

16. **Gupta S, Feng L, Yoshimura T, Redick J, Fu SM and Rose CE, Jr.** Intra-alveolar macrophage-inflammatory peptide 2 induces rapid neutrophil localization in the lung. *Am J Respir Cell Mol Biol* 15: 656-663, 1996.

17. **Han L, Saito H, Fukatsu K, Inoue T, Yasuhara H, Furukawa S, Matsuda T, Lin MT and Ikeda S**. Ex vivo fluorescence microscopy provides simple and accurate assessment of neutrophil-endothelial adhesion in the rat lung. *Shock* 16: 143-147, 2001.

18. **Hanger CC, Wagner WW, Jr., Janke SJ, Lloyd TC, Jr. and Capen RL**. Computer simulation of neutrophil transit through the pulmonary capillary bed. *J Appl Physiol* 74: 1647-1652, 1993.

19. **Henderson RB, Hobbs JAR, Mathies M and Hogg N**. Rapid recruitment of inflammatory monocytes is independent of neutrophil migration. *Blood* 102: 328-335, 2003.

20. **Hermanns MI, Unger RE, Kehe K, Peters K and Kirkpatrick CJ**. Lung epithelial cell lines in coculture with human pulmonary microvascular endothelial cells: development of an alveolo-capillary barrier in vitro. *Lab Invest* 84: 736-752, 2004.

21. **Huang Y, Doerschuk CM and Kamm RD**. Computational modeling of RBC and neutrophil transit through the pulmonary capillaries. *J Appl Physiol* 90: 545-564, 2001.

22. **Kina T, Ikuta K, Takayama E, Wada K, Majumdar AS, Weissman IL and Katsura Y**. The monoclonal antibody TER-119 recognizes a molecule associated with glycophorin A and specifically marks the late stages of murine erythroid lineage. *Br J Haematol* 109: 280-287, 2000.

23. **Li Q, Park PW, Wilson CL and Parks WC**. Matrilysin shedding of syndecan-1 regulates chemokine mobilization and transepithelial efflux of neutrophils in acute lung injury. *Cell* 111: 635-646, 2002.

24. **Lorenz E, Jones M, Wohlford-Lenane C, Meyer N, Frees KL, Arbour NC and Schwartz DA**. Genes other than TLR4 are involved in the response to inhaled LPS. *Am J Physiol Lung Cell Mol Physiol* 281: L1106-L1114, 2001.

25. **Mackarel AJ, Russell KJ, Ryan CM, Hislip SJ, Rendall JC, FitzGerald MX and O'Connor CM**. CD18 dependency of transendothelial neutrophil

migration differs during acute pulmonary inflammation. *J Immunol* 167: 2839-2846, 2001.

26. **Markowicz P, Wolff M, Djedaini K, Cohen Y, Chastre J, Delclaux C, Merrer J, Herman B, Veber B, Fontaine A and Dreyfuss D**. Multicenter prospective study of ventilator-associated pneumonia during acute respiratory distress syndrome. Incidence, prognosis, and risk factors. ARDS Study Group. *Am J Respir Crit Care Med* 161: 1942-1948, 2000.

27. **Matthay MA, Zimmerman GA, Esmon C, Bhattacharya J, Coller B, Doerschuk CM, Floros J, Gimbrone MA, Jr., Hoffman E, Hubmayr RD, Leppert M, Matalon S, Munford R, Parsons P, Slutsky AS, Tracey KJ, Ward P, Gail DB and Harabin AL**. Future research directions in acute lung injury: summary of a National Heart, Lung, and Blood Institute working group. *Am J Respir Crit Care Med* 167: 1027-1035, 2003.

28. **Maus UA, Waelsch K, Kuziel WA, Delbeck T, Mack M, Blackwell TS, Christman JW, Schlondorff D, Seeger W and Lohmeyer J**. Monocytes are potent facilitators of alveolar neutrophil emigration during lung inflammation: role of the CCL2-CCR2 axis. *J Immunol* 170: 3273-3278, 2003.

29. **Miller EJ, Cohen AB, Nagao S, Griffith D, Maunder RJ, Martin TR, Weiner-Kronish JP, Sticherling M, Christophers E and Matthay MA**. Elevated levels of NAP-1/interleukin-8 are present in the airspaces of patients with the adult respiratory distress syndrome and are associated with increased mortality. *Am Rev Respir Dis* 146: 427-432, 1992.

30. **Moreland JG, Bailey G, Nauseef WM and Weiss JP**. Organism-specific neutrophil-endothelial cell interactions in response to Escherichia coli, Streptococcus pneumoniae, and Staphylococcus aureus. *J Immunol* 172: 426-432, 2004.

31. **Olson TS, Singbartl K and Ley K**. L-selectin is required for fMLP- but not C5a-induced margination of neutrophils in pulmonary circulation. *Am J Physiol Regul Integr Comp Physiol* 282: R1245-R1252, 2002.

32. **Peng X, Hassoun PM, Sammani S, McVerry BJ, Burne MJ, Rabb H, Pearse D, Tuder RM and Garcia JGN**. Protective Effects of Sphingosine 1-Phosphate in Murine Endotoxin-induced Inflammatory Lung Injury. *Am J Respir Crit Care Med* 169: 1245-1251, 2004.

33. **Pruijt JFM, Verzaal P, van Os R, de Kruijf EJ, van Schie MLJ, Mantovani A, Vecchi A, Lindley IJD, Willemze R, Starckx S, Opdenakker G and Fibbe WE**. Neutrophils are indispensable for hematopoietic stem cell mobilization induced by interleukin-8 in mice. *PNAS* 99: 6228-6233, 2002.

34. **Puneet P, Moochhala S and Bhatia M**. Chemokines in acute respiratory distress syndrome. *Am J Physiol Lung Cell Mol Physiol* 288: L3-L15, 2005.

35. **Razavi HM, Wang LF, Weicker S, Rohan M, Law C, McCormack DG and Mehta S**. Pulmonary Neutrophil Infiltration in Murine Sepsis: Role of Inducible Nitric Oxide Synthase. *Am J Respir Crit Care Med* 170: 227-233, 2004.

36. **Reutershan J and Ley K**. Bench-to-bedside review: Acute respiratory distress syndrome - how neutrophils migrate into the lung. *Crit Care* 8: 453-461, 2004.

37. **Sato Y, Van Eeden SF, English D and Hogg JC**. Bacteremic pneumococcal pneumonia: bone marrow release and pulmonary sequestration of neutrophils. *Crit Care Med* 26: 501-509, 1998.

38. **Schwab AJ, Salamand A, Merhi Y, Simard A and Dupuis J**. Kinetic analysis of pulmonary neutrophil retention in vivo using the multiple-indicator-dilution technique. *J Appl Physiol* 95: 279-291, 2003.

39. **Sikora L, Johansson AC, Rao SP, Hughes GK, Broide DH and Sriramarao P**. A murine model to study leukocyte rolling and intravascular trafficking in lung microvessels. *Am J Pathol* 162: 2019-2028, 2003.

40. **Skerrett SJ, Liggitt HD, Hajjar AM, Ernst RK, Miller SI and Wilson CB**. Respiratory epithelial cells regulate lung inflammation in response to inhaled endotoxin. *Am J Physiol Lung Cell Mol Physiol* 287: L143-L152, 2004.

41. **Smith ML, Olson TS and Ley K**. CXCR2- and E-Selectin-induced Neutrophil Arrest during Inflammation In Vivo. *J Exp Med* 200: 935-939, 2004.

42. **Sue RD, Belperio JA, Burdick MD, Murray LA, Xue YY, Dy MC, Kwon JJ, Keane MP and Strieter RM**. CXCR2 is critical to hyperoxia-induced lung injury. *J Immunol* 172: 3860-3868, 2004.

43. **Tasaka S, Qin L, Saijo A, Albelda SM, DeLisser HM and Doerschuk CM**. Platelet endothelial cell adhesion molecule-1 in neutrophil emigration during acute bacterial pneumonia in mice and rats. *Am J Respir Crit Care Med* 167: 164-170, 2003.

44. **Wagner JG, Harkema JR and Roth RA**. Pulmonary leukostasis and the inhibition of airway neutrophil recruitment are early events in the endotoxemic rat. *Shock* 17: 151-158, 2002.

45. **Wang LF, Patel M, Razavi HM, Weicker S, Joseph MG, McCormack DG and Mehta S**. Role of Inducible Nitric Oxide Synthase in Pulmonary Microvascular Protein Leak in Murine Sepsis. *Am J Respir Crit Care Med* 165: 1634-1639, 2002.

46. **Yamada M, Kubo H, Kobayashi S, Ishizawa K, Numasaki M, Ueda S, Suzuki T and Sasaki H**. Bone marrow-derived progenitor cells are important for lung repair after lipopolysaccharide-induced lung injury. *J Immunol* 172: 1266-1272, 2004.

Figure 1: LPS-inhalation induces a time dependent recruitment of leukocytes and PMN into the lung (**A**) and BAL (**B**). X-axis indicates time after LPS exposure. Absolute numbers of leukocytes ($CD45^+$) and PMN ($CD45^+GR\text{-}1^+7/4^+$) were obtained as the product of flow cytometry percentage and hemocytometer-based total cell counts. Data are presented as mean ± SEM of n = 4 experiments at each time point.

Figure 2: In-vivo anti-GR-1 labeling. 10µg rat anti-mouse GR-1 was injected and blood was taken five minutes later. PMN were identified by their typical appearance in the forward-sideward scatter (**A**) and by the expression of 7/4 antigen. GR-1 labeling in these cells was determined (**B**). Five minutes after antibody injection, almost all PMN (>99%) were GR-1+. Plot shows a representative result of n = 6 experiments. Panel **C** and **D**: GR-1 labeling in BAL. At different time points after LPS-exposure, 10µg rat anti-mouse GR-1 was injected and BAL performed five minutes thereafter. PMN were identified by expression of CD45 and 7/4. No GR-1+ cells were found in the BAL (**C**). Panel **D** shows the positive control (BAL stained with anti-GR-1 and anti-7/4 after harvesting). Graphs show representative dot plot 24h after LPS-exposure.

Figure 3: In-vivo PMN trafficking. **A**: PMN numbers in the different lung compartments 0, 1, 2, 4, 12, and 24 hours after LPS-exposure. GR-1 antibody was injected five minutes prior to euthanasia. PMN were identified as $7/4^+$. GR-1 labeling was used to distinguish between intravascular ($GR\text{-}1^+$; right upper

quadrants; UR) and interstitial (GR-1$^-$; right lower quadrants; LR) PMN. PMN accumulation in the pulmonary vasculature started rapidly after LPS-exposure and reached a peak after 4 hours. Significant migration into the interstitial space started between 2 and 4 hours after LPS-exposure, increased continuously, and reached a plateau after 12 hours. Percent interstitial PMN indicated in lower right square. **B**: PMN in BAL. Initial PMN concentration at t=0h is negligible. A significant increase in PMN concentration appears between 2 and 4 hours. PMN in the BAL do not stain for GR-1 as this antibody has been injected i.v. and does not reach the alveolar airspace. Graphs are representative of n = 4 time course experiments.

Figure 4: Time course of PMN trafficking. At 0, 1, 2, 4, 12, and 24 hours after LPS-exposure, PMN concentrations were assessed in the different lung compartments (vasculature, interstitium, BAL). Pulmonary circulation was flushed to remove non-adherent cells. Absolute PMN counts were calculated by total leukocyte counts (Trypan Blue exclusion) and relative PMN concentrations obtained by flow cytometry. Mean ± SEM of n = 4 time course experiments are displayed. Asterisks indicate significant difference in cell count from baseline at t=0h. **Insets**: Cytospin of BAL at t=0h (**a**) and t=24h (**b**). BAL of untreated mice was dominated by alveolar macrophages. 24 hours after LPS-inhalation, the cell population changed to predominantly PMN.

Figure 5: To confirm lung injury in response to LPS inhalation, vascular permeability in the lung was determined using the Evans blue extravasation technique. 6 hours after LPS inhalation, Evans blue extravasation into the lung was significantly higher compared to the control group which had received saline inhalation (66.2 ± 6.2 vs. 29.3 ± 3.7 µg Evans blue per g lung; p = 0.002). Data are presented as mean ± SEM of n = 4 animals in each group.

Figure 6: To block Gαi-dependent signaling, PTx was injected 30 minutes prior to LPS challenge. PMN in lungs and BAL were assessed 14 hours after LPS-exposure. Anti GR-1-antibody was injected five minutes prior to euthanasia. PMN were identified by their expression of CD45 and 7/4. GR-1 was utilized to distinguish intravascular ($GR\text{-}1^{+}$) and interstitial ($GR\text{-}1^{-}$) PMN. LPS induced a significant PMN recruitment to all three compartments of the lung. PTx pretreatment sharply reduced PMN migration into the interstitium and almost completely eliminated PMN recruitment into the alveolar airspace. In contrast, PMN counts in the vascular compartment remained unaffected. **A**: Representative facs plot of n = 3 experiments. **B**: Absolute PMN counts in the different compartments of the lung (open bars: control; black bars: LPS; hatched bars: LPS + PTx). Asterisks indicate significant difference in PMN counts from the control. Data are presented as mean ± SEM of n = 3 experiments in each group.

Figure 7: PTx induced a dose-dependent inhibition of PMN-migration into BAL (**A**) and interstitial space (**B**). PTx was injected i.v. 30 minutes prior to LPS-exposure. PMN in the different lung compartments were determined after 12 hours. No effect of PTx on PMN-recruitment into the pulmonary vasculature was observed (**C**).

Table 1: In vivo neutrophil labeling

	$7/4^+$ (%) *	GR-$1^+7/4^+$ (%) *	n (mice)
Blood	99.6 ± 0.3%	99.2 ± 0.4%	6
BAL	90.5 ± 5.3%	0.14 ± 0.1%	6

* Anti-7/4 was added after harvesting; anti-GR-1 was injected i.v.

Figure 1

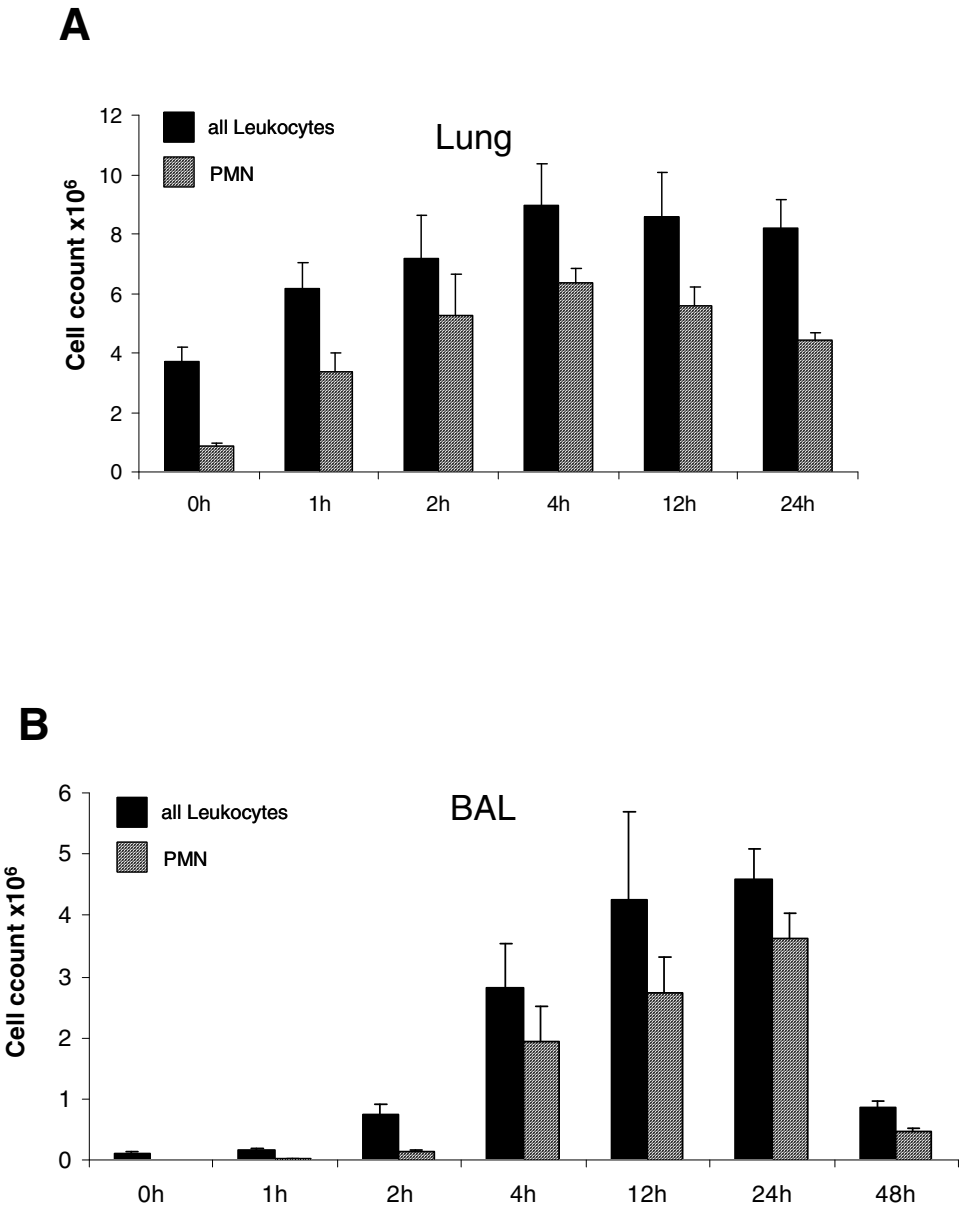
A
all Leukocytes
PMN
Lung
Cell ccount x10^6
12
10
8
6
4
2
0
0h
1h
2h
4h
12h
24h
B
all Leukocytes
PMN
BAL
Cell ccount x10^6
6
5
4
3
2
1
0
0h
1h
2h
4h
12h
24h
48h

Figure 2

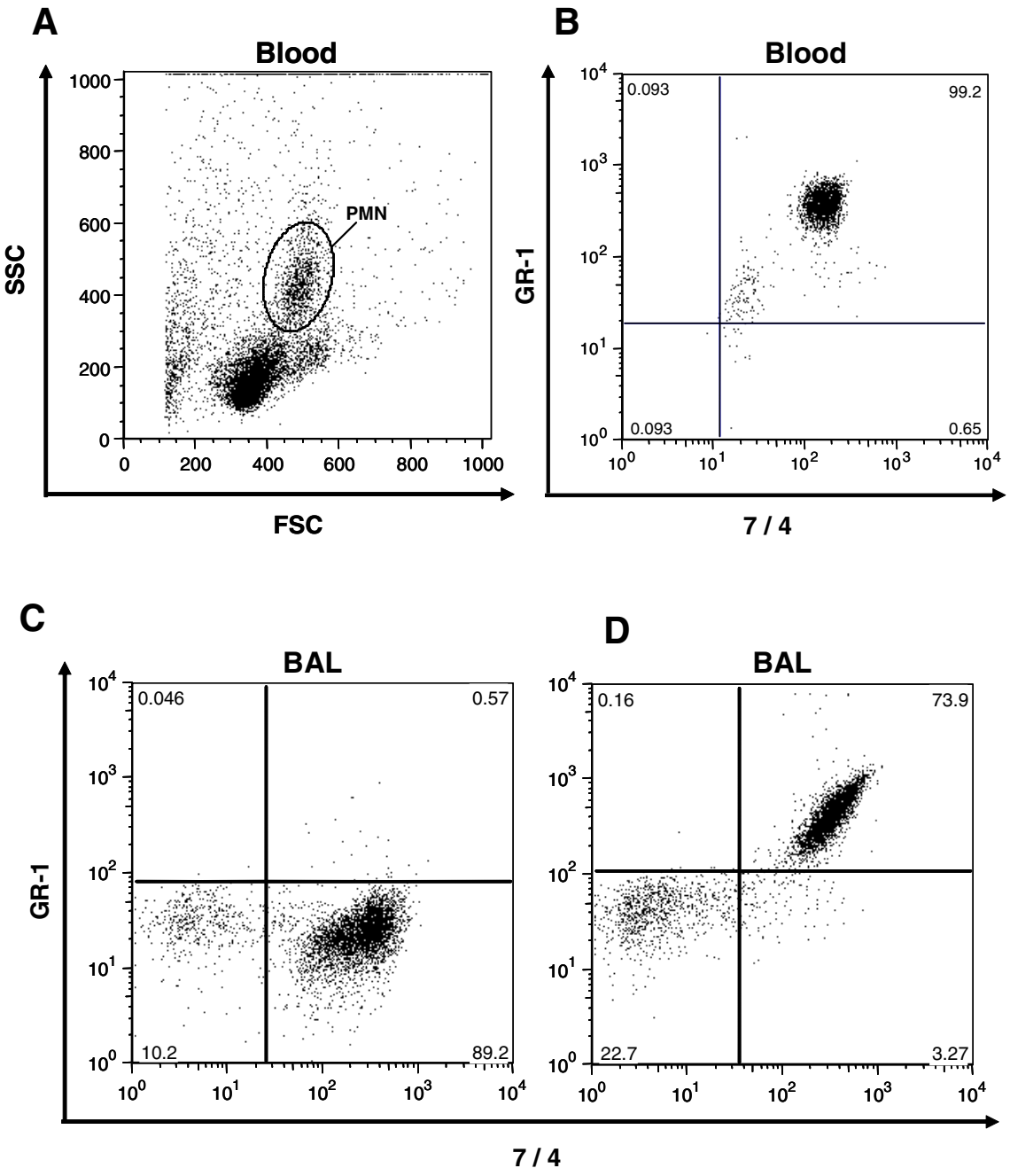
A
Blood
SSC
FSC
PMN
B
Blood
GR-1
7 / 4
0.093
99.2
0.093
0.65
C
BAL
GR-1
7 / 4
0.046
0.57
10.2
89.2
D
BAL
0.16
73.9
22.7
3.27

Figure 3

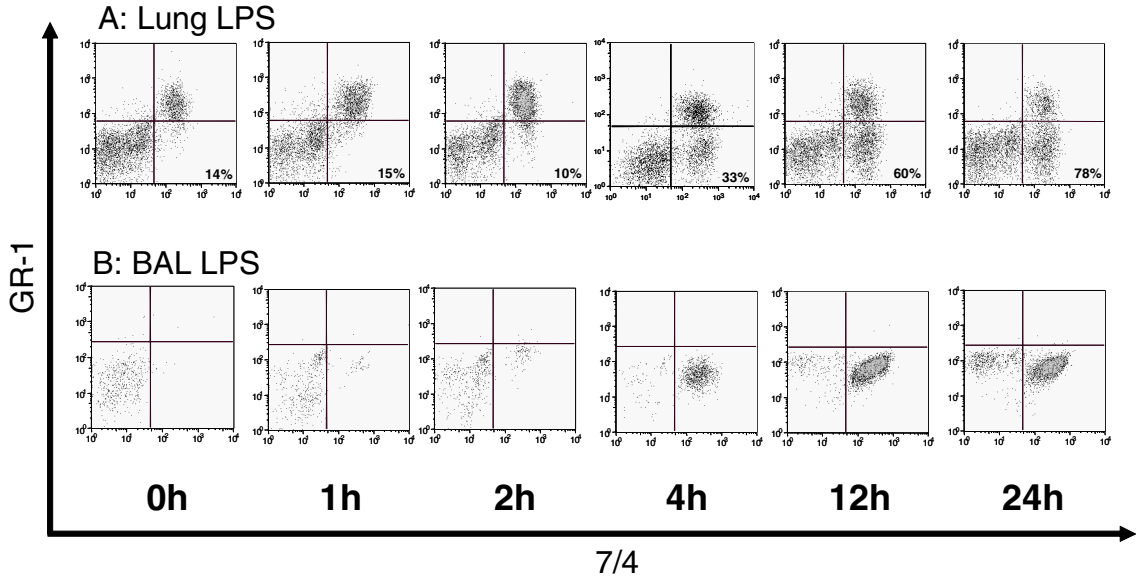

Figure 4

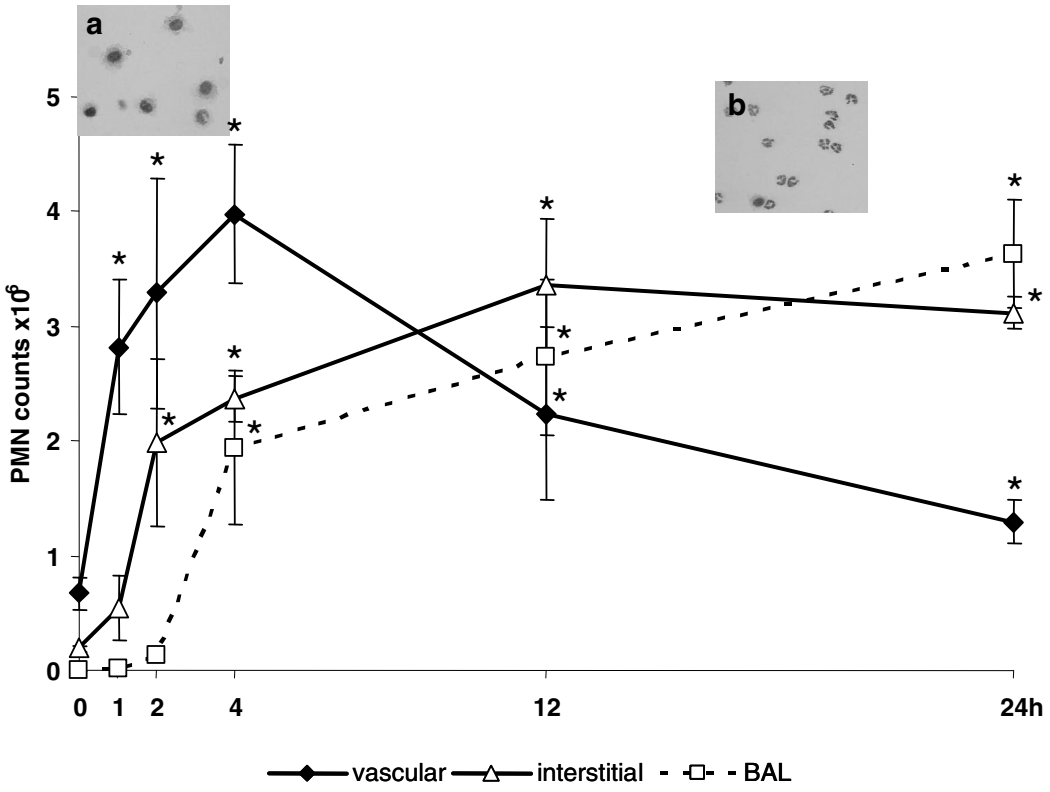
a
b
PMN counts x10^6
0
1
2
3
4
5
0
1
2
4
12
24h
vascular
interstitial
BAL

Figure 5

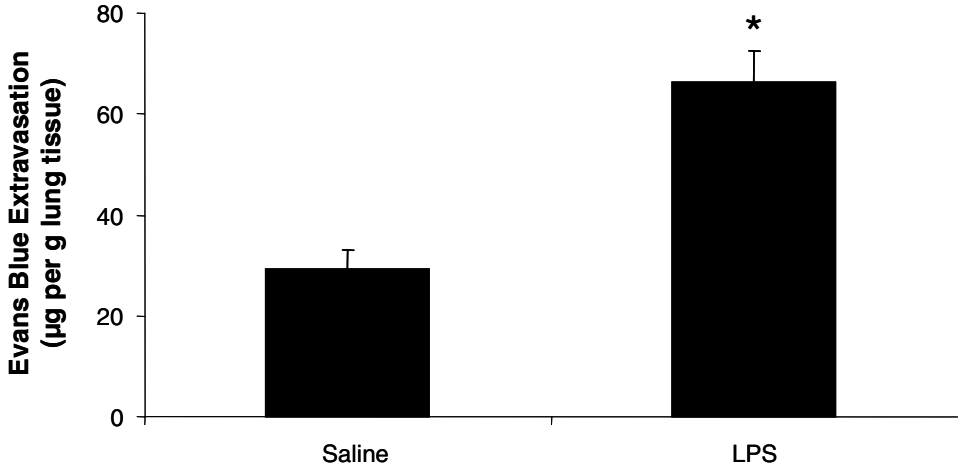
Evans Blue Extravasation
(µg per g lung tissue)
80
60
40
20
0
*
Saline
LPS

Figure 6

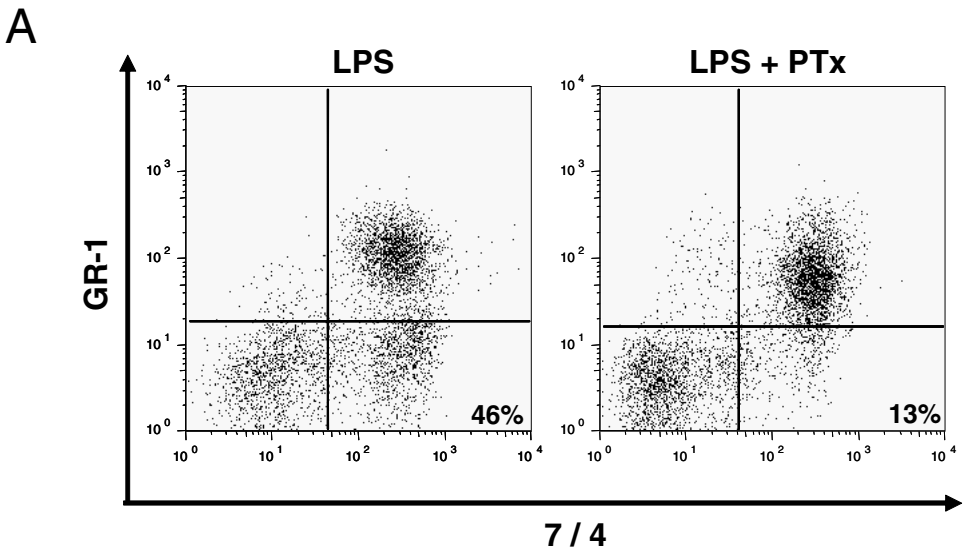
A
LPS
LPS + PTx
GR-1
7 / 4
46%
13%

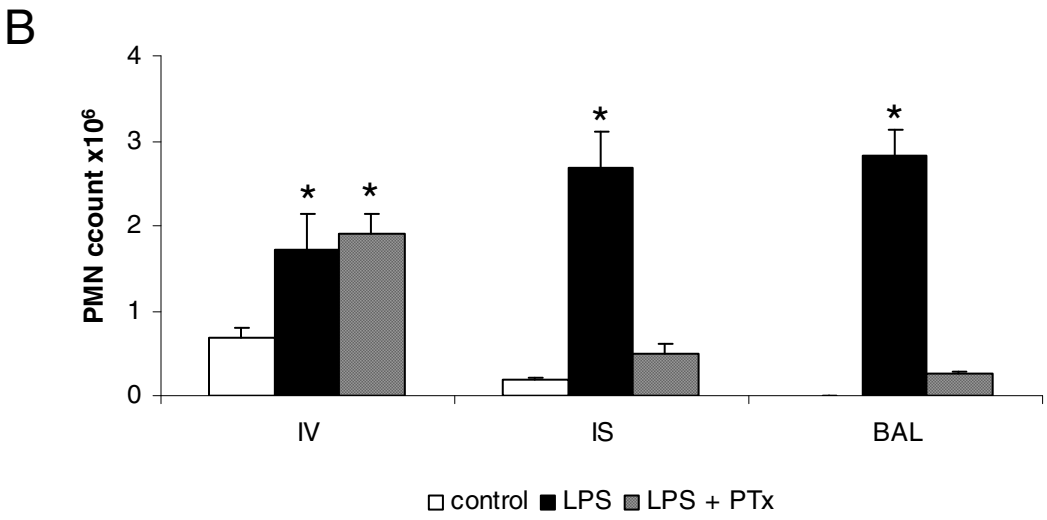
B
PMN ccount x10⁶
IV
IS
BAL
control
LPS
LPS + PTx

Figure 7

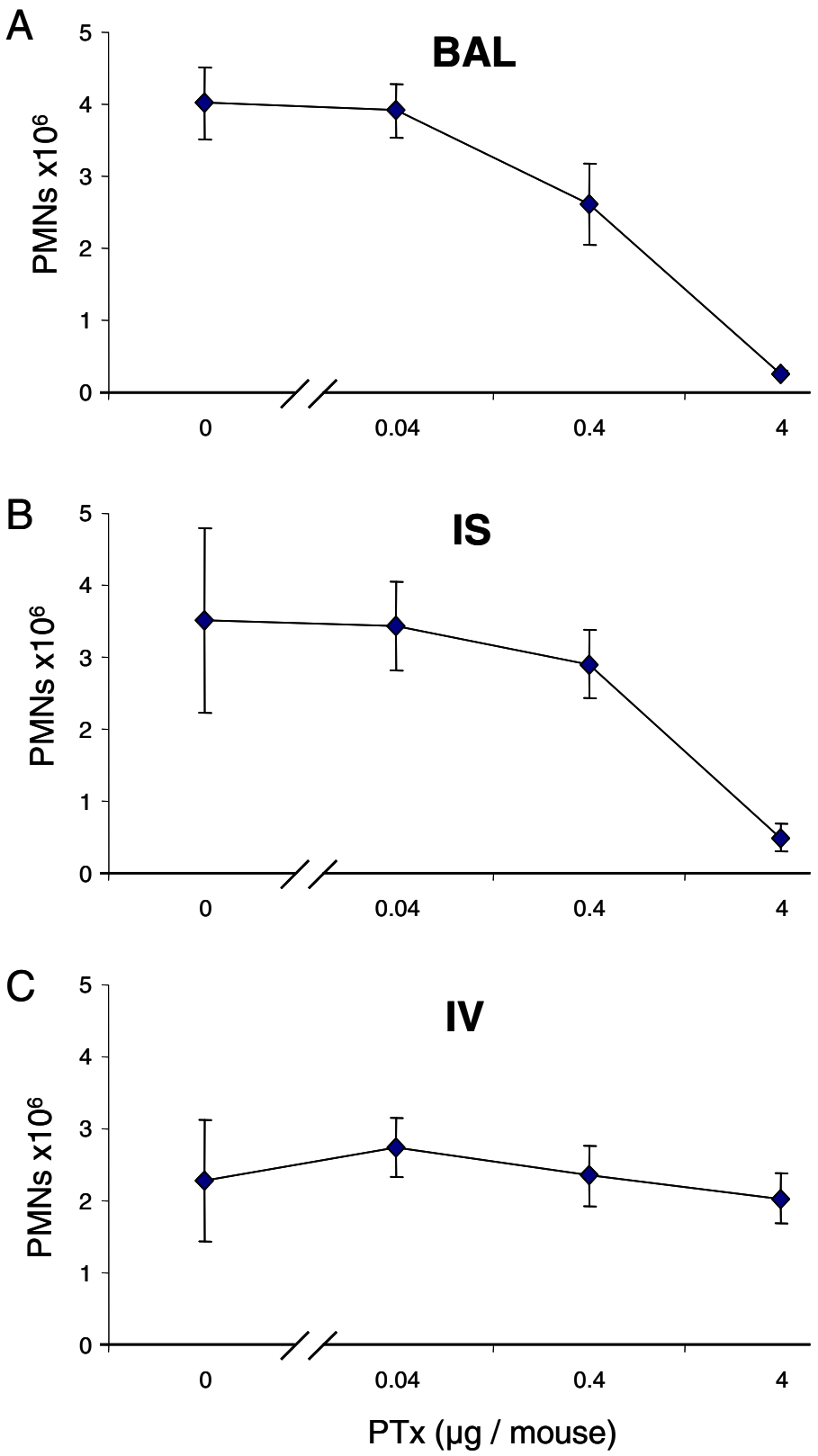
A
BAL
PMNs x10⁶
5
4
3
2
1
0
0
0.04
0.4
4
B
IS
PMNs x10⁶
5
4
3
2
1
0
0
0.04
0.4
4
C
IV
PMNs x10⁶
5
4
3
2
1
0
0
0.04
0.4
4
PTx (µg / mouse)